Influence of Toluene on the Bending Elastic Properties of Giant Phosphatidylcholine Vesicles

E. Brückner, P. Sonntag, and H. Rehage*

Institute of Physical Chemistry, University of Essen, Essen D-45141, Germany

Received: September 14, 1999

In the present study the influence of toluene on the bending elastic modulus k_c of dimyristoylphosphatidylcholine (DMPC) vesicles in the L_α phase is investigated using videomicroscopy. For giant unilamellar DMPC vesicles, a mean value of $k_c = (1.42 \pm 0.21) \times 10^{-19}$ J is determined at 30 °C. Addition of toluene, which is predominantly incorporated in the lipophilic core of the bilayer, induces a lowering of the bending elastic modulus with increasing concentration up to a plateau value of $k_c = (0.36 \pm 0.10) \times 10^{-19}$ J. This effect seems to be dominated by the mobility of the nonpolar molecules in the lipophilic part of the bilayer. Vesicles near the maximum solubilization capacity exhibit an anomalous increase of the bending elastic constant because of the formation of small hydrophobic clusters of phase-separated toluene. In the case of complete membrane saturation, these clusters can be clearly visualized in the vesicle membrane region. Thermally induced undulations vanish as a consequence of the reduction of the excess area Δ. Microscopy investigations of the temperature dependence of the bending elastic modulus were performed for both pure DMPC and toluene containing DMPC vesicles. Further analysis of the isobaric thermal area expansion coefficient β indicates a reduced thermal expansivity for vesicles containing toluene. The values of β vary from $(6.9 \pm 0.8) \times 10^{-3}$ K^{-1} for DMPC vesicles to $(1.6 \pm 0.3) \times 10^{-3}$ K^{-1} in the presence of toluene.

Introduction

Amphiphilic molecules in aqueous solution tend to build up bilayer membranes, which in turn can form multi- or unilamellar vesicles. These structures are relevant for a broad field of research ranging from theoretical modeling of biological membranes to numerous medical as well as nonmedical applications (e.g., remediation of contaminated soils).[1,2] As a simple model for biological membranes, vesicles allow one to study cellular stability and shape transitions.[3,4] Passive transport processes such as, for example, of anesthetic drugs through the cell membrane and possible pathways of cellular damage could be analyzed using vesicular structures.[5,6] Because of their ability to encapsulate part of the aqueous environment, liposomes have attracted current interest in cosmetic or pharmaceutical applications as a drug carrier.[7] Moreover, vesicles appear to have applications in material science. An advanced technique uses the lipophilic core of the bilayer as a template for polymerization[8,9] in order to form hollow spheres of polymer after the removal of the amphiphile.[10,11]

Compared to isotropic bulk phases, the properties of bilayers are different because of the high surface-to-volume ratios.[12] Contrary to droplets where the shape is mainly determined by the surface tension, the shape of a vesicle is fixed by the area and volume constraints. These constraints arise from the small solubility of the lipid molecules in the water phase and the slow flip−flop rates. The thin and soft membrane is easy to bend but difficult to stretch or compress. The bending energy, which is in the range of $10-50kT$ for membranes in the fluid L_α phase,[13−15] controls the fluctuations of a vesicle from one shape to another. Hence, videomicroscopy investigations of the fluctuations of giant quasi-spherical vesicles originating from Brownian motion can be used to evaluate the elastic properties such as the effective tension $\bar{\sigma}$ and the bending rigidity k_c.[13,16] While the first is more a geometric property of the vesicle, the bending rigidity describes a membrane elastic property. It determines the amplitude of the undulations of the membrane and rules the steric interaction between bilayers or vesicles and surfaces.[17] It also plays a key role in adhesion of vesicles.[18] Furthermore, the rate of permeation through porous media like the mammalian skin was shown to be dependent on the bending elastic constant.[19] Thus, the knowledge of k_c is important to understand the dynamic features of liposomes.

Because the physical properties of the membrane are very sensitive to the composition, partitioning of solutes into the lipid bilayer may significantly alter elastic parameters. Therefore, many investigations, mainly focused on the biophysical aspects, have been reported on the elastic properties of giant vesicles. Usually, natural phospholipids such as egg lecithin or synthetic lecithins such as 1,2-dimyristoyl-*sn*-phosphatidylcholine (DMPC) in the fluid state composed the vesicle structure. A great variety of techniques was used for the determination of the bending elastic constant of giant unilamellar vesicles. Invasive techniques such as the micropipet aspiration[20,21] or the elongation of quasi-spherical vesicles in an ac electric field[15,22] as well as noninvasive techniques such as the flicker experiments[16,23] or synchrotron X-ray scattering[24] have been applied. It was found that the interactions of the lipids with a diversity of surface-active compounds significantly influence the elastic behavior of the bilayer.

The most popular example is cholesterol, which is known to be a regulator of the fluidity of eucariotic cell membranes. Cholesterol was shown to enhance the bending rigidity k_c when incorporated in the membrane of DMPC vesicles.[25,26] This increase should be due to an "ordering effect" on the fluid phase of the lipid.[26]

The addition of substances such as short-chain lipids,[27,28] alcohols,[24] bola lipids,[29,30] or proteins, like the ion-carrier

10.1021/jp993265c CCC: $19.00
Published on Web 02/18/2000

valinomycin,[31] was found to cause a reduction of the bending elasticity compared to the pure DMPC. This effect can be attributed either to the "spacer" function of the short-chain lipids[27] or to a modification of the thickness of the membrane as seen for pure phospholipids of variable chain length.[14] A further explanation relies on a coupling between the local curvature and the intercalated molecules[32] which is related to a difference in the packing parameter between the phospholipid and the incorporated compound.

Most of these effects are prone to be concentration-dependent and may be very efficient. For example, upon addition of cosurfactants such as the "edge-active" sodium cholate, ultraflexible liposomes, the so-called transfersomes, can be obtained. These transfersomes have been reported to show high permeability for porous media like the mammalian skin.[33]

All of these investigations focused on substances that may act as cosurfactants having a high affinity to the headgroup region of the phospholipids. Less is known about the influence of lipophilic compounds on the elastic properties of the bilayer. Only Niggemann et al.[22] indicated that the accumulation of xylene from the sample cell sealing into the bilayer could lead to a decrease of k_c. Hence, the aim of our investigation was the examination of the influence of toluene as a nonpolar additive to phospholipids on the bending elastic constant. Moreover, we tried to correlate the mechanical behavior to features on the molecular level.

Theoretical Background

The first attempt to deduce the bending elastic modulus from shape fluctuations of unilamellar quasi-spherical vesicles was made by Schneider et al. in 1984.[23] These ideas were further improved by Milner and Safran.[34] Their model is based on a second-order expansion of the deviation of the vesicle shape from a sphere in terms of three-dimensional spherical harmonics. The amplitudes of the spherical harmonics are expressed as a function of the bending elastic constant and the effective tension $\bar{\sigma}$.[34]

Because microscopy experiments only deliver information about the fluctuations of the median contour, the expression provided by the theory has to be adapted. Two approaches have been used. In the first a Fourier decomposition of the observed contour is made and the amplitudes of the various modes are expressed as a complex sum of the amplitudes of the spherical harmonics.[25]

The slightly deformed vesicle is then described in polar coordinates (ρ, φ) by

$$\rho(\varphi,t) = R_0(1 + u(\varphi,t)) \tag{1}$$

where $u(\varphi,t)$ is the relative displacement of the membrane with respect to the projection of a sphere with equivalent volume and the radius R_0. Denoting $\nu_q(t)$ as the time-dependent amplitudes obtained from the Fourier analysis of $u(\varphi,t)$, one has

$$\nu_q(t) = \frac{1}{2\pi}\int_0^{2\pi} u(\varphi,t)\, e^{iq\varphi}\, d\varphi \tag{2}$$

The bending elastic constant can then be expressed as[25]

$$k_c = \frac{kT}{\langle|\nu_q|^2\rangle}\sum_{l=q}^{l_{max}} \frac{2l+1}{4\pi}\frac{(l-q)!}{(l+q)!}\frac{[P_l^q(\cos \pi/2)]^2}{(l-1)(l+2)[l(l+1)+\bar{\sigma}]} \tag{3}$$

where P_l^q are the associated Legendre polynomials, k is the Boltzmann constant, and $\bar{\sigma}$ is the effective tension. The bending elastic constant and the effective tension can then be deduced by performing a fit of ν_q as a function of the wavenumber q. This procedure is nontrivial because the effective tension appears in the sum. Thus, for the determination of the bending elastic constant, the influence of $\bar{\sigma}$ is often neglected.[14,25]

A further approach uses the properties of the angular autocorrelation function of the contour defined as[13]

$$\xi(\gamma,t) = \frac{1}{R_0^2}\left[\frac{1}{2\pi}\int \rho(\varphi+\gamma,t)\,\rho^*(\varphi,t)\, d\varphi - \bar{\rho}^2(t)\right] \tag{4}$$

$\bar{\rho}$ denotes the average radius.

The autocorrelation function can be decomposed in a series of Legendre polynomials according to

$$\langle\xi(\gamma,t)\rangle = \sum_{l=2}^{l_{max}} B_l(\bar{\sigma},k_c)\, P_l(\cos\gamma) \tag{5}$$

The amplitudes of this decomposition are related to the amplitudes of the spherical harmonics.[13] The bending elastic constant is then obtained by the following equation:

$$B_l(\bar{\sigma},k_c) = \frac{kT}{4\pi k_c}\frac{2l+1}{(l-1)(l+2)[\bar{\sigma}+l(l+1)]} \tag{6}$$

A fit is still necessary to obtain the value of the bending elastic constant and the effective tension, but this procedure is less complex than that for the Fourier analysis.

The effective tension arising in the expressions should be considered carefully. It has been introduced in the equations as a Lagrange multiplier in order to ensure area conservation.[23,34,35] In fact, more detailed calculations treating the area conservation exactly show that the amplitude of the fluctuations depends only on the bending elastic constant and the excess surface.[36] Therefore, instead of this apparent tension, one has to consider the excess surface area Δ which is the physically meaningful variable. This latter is a measurable quantity defined by

$$A = 4\pi R_0^2(1 + \Delta) \tag{7}$$

where A is the surface of the vesicle and R_0 is the radius of the equivalent sphere. The relation between the apparent effective tension and the excess area is given by the implicit equation[37]

$$\Delta(T) = \frac{kT}{8\pi k_c}\sum_{l\geq 2}^{l_{max}}\frac{2l+1}{l(l+1)+\bar{\sigma}} \tag{8}$$

Negative values of the effective tension are also possible and can be interpreted as a vesicle with a quite large excess surface. The model holds for values up to $\bar{\sigma} \approx -6$ where the vesicle becomes ellipsoidal.

Materials and Methods

Synthetic DMPC and toluene were purchased from Fluka (Biochemika). Both compounds had a purity of 99% or greater and were used without further treatment. The water employed in this study was deionized with a Millipore system. After filtration through a 0.2 μm pore size sterile filter (Minisart, Sartorius), the water was degassed and purged with argon.

Giant vesicles were prepared according to the swelling method of Reeves and Dowben[38] as reported previously.[39] The dispersion consisting of uni- and multilamellar vesicles was transferred to airtight glass bottles and quickly sealed using a

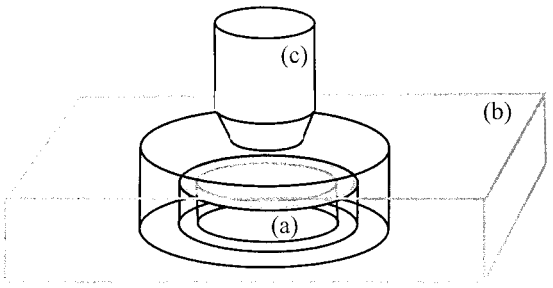

Figure 1. Schematic view of the thermal stage including the observation chamber: (a) quartz microchamber, (b) thermoblock, (c) objective.

Teflon-lined cap to prevent gas leakage after addition of toluene. The samples were gently shaken for about 1 min to avoid formation of emulsion droplets and stored at 30 °C for several hours. The yield of ideal (unilamellar) vesicles is significantly lower compared to the electropreparation method,[40] but this technique allows one to avoid toluene evaporation.

Investigations were performed in dilute aqueous solutions with total lipid concentrations of 1 mM. For the microscopy observations, a small amount of the dispersion was placed in an observation microchamber having a total volume of 36 μL and a light path of 0.2 mm. The chamber was covered with a quartz coverslip. The use of any type of grease, silicon paste, or plastic material was avoided because of a possible interaction with the lipid membrane and its influence on the bending elasticity.[22] The samples were kept at constant temperature for about 3 h prior to investigation using the thermostat chamber shown in Figure 1. During this period a sedimentation, especially of the multilamellar vesicles, can be observed. Only the remaining free fluctuating vesicles in the aqueous solution were used to determine the bending elastic modulus. Measurements were performed at 30 °C which is about 7 K above the gel-to-liquid transition temperature ($P_{\beta'} \rightarrow L_\alpha$) of DMPC vesicles.[41] Thus, influences due to anomalous behavior of k_c near the phase transition could be avoided.[14]

Microscopy. Vesicle observation was performed using a phase-contrast microscope BX-50 (Olympus Optical Co.) with a 40× objective (Ph 2, NA = 0.75).

Phase-contrast microscopy has been shown to be a common method for the extraction of contour coordinates from freeze frame images of a fluctuating vesicle.[42] Despite the disadvantage of comparably low resolution, it prevails over the difficulties of other techniques such as the Nomarski differential contrast[16] or fluorescence microscopy.[23]

Black and white images of the fluctuations were taken with 12 bit gray level resolution using a cooled CCD camera (Sensi Cam, PCO). The exposure time was set at 10 ms. The time interval between the images, usually 1 s, was tested to be long enough to neglect correlation of the slow fluctuation modes. Images were stored on a hard disk of a personal computer (Pentium 233 MHz) for further contour extractions.

Image processing and contour extraction was performed using Optimas 6.0 (Stemmer Imaging) and applying the algorithm given by Liu.[43] Typically vesicles with radii of 10−20 μm were observed.

Microscopical investigations were performed on single vesicles under dilute conditions. To determine the approximate molar ratio toluene/DMPC of the observed unilamellar vesicles, the partition coefficients for the respective concentration were deduced. Partition measurements were carried out according to the method described by Katz and Diamond.[44] Multilamellar liposomes of DMPC (1 mM) were incubated with different amounts of toluene for about 6 h by shaking in a gastight bottle at 30 °C. Afterward the dispersion was centrifuged at 30 °C with a temperature-controlled Beckman centrifuge (J2-HS) for 1 h at 20 000*g*. The concentration of toluene in the clear supernatant was measured using a Varian UV−visible spectrophotometer (Cary 1 E). The amount of toluene in the vesicles was determined from the reduction of toluene in the aqueous solution.

Data Representation and Error Determination. When using the autocorrelation function, the bending elastic constant is usually deduced by a direct fit of eq 6. The anomalies and systematic deviation that may then occur can only be detected by statistical tests. To overcome this complicated procedure, we have rewritten the relation between B_l and the bending elastic constant in a more convenient form

$$U_l(\bar{\sigma},k_c) = k_c\bar{\sigma} + k_c l(l+1) \tag{9}$$

where $U_l(\bar{\sigma},k_c)$ is defined as

$$U_l(\bar{\sigma},k_c) = \frac{kT}{4\pi}\frac{2l+1}{(l-1)(l+2)B_l(\bar{\sigma},k_c)} \tag{10}$$

Equation 10 shows that the representation of $U_l(\bar{\sigma},k_c)$ as a function of $l(l+1)$ should present a linear behavior. The bending elastic constant is then deduced from the slope of the data. The crossing of the interpolated line and the *y* axis gives the effective tension. The main interest of this representation is that deviations to the normal behavior can be checked visually without any fitting procedure. On grounds of this advantage, we favor the $U_l(\bar{\sigma},k_c)$ vs $l(l+1)$ plot to extract the value of the effective tension. This parameter can then further be used for the exact determination of the dependence of k_c on the wavevector q, allowing anomalies in the small q domain to be corrected. Values of the bending elastic constants obtained by the two procedures were compared for agreement. The use of the two methods seems to be a simple way of checking experimental aberrations and the consistency of the results obtained. The validity of the theoretical model was checked by numerical simulation as described before.[35]

Error-weighted fits were performed using a standard Minsq routine (Micromath). The experimental errors on the amplitudes of the Fourier modes and of the Legendre modes were given by the mean-square deviation.

X-ray Diffraction. X-ray diffraction studies were performed using a fully hydrated dispersion of DMPC with 40 wt % water at different toluene-to-lipid molar ratios. Measurements were carried out at $T = 25 \pm 1$ °C in the L_α phase of DMPC. The samples were placed in 2 mm × 80 mm quartz capillaries and equilibrated after sealing. The X-ray source was a Siemens Krystalloflex generator equipped with a fine focus tube. The Cu Kα radiation with a wavelength $\lambda = 0.154\,06$ nm was filtered using a quartz monochromator. Data were collected using a Siemens D5000 diffractometer equipped with a scintillation counter. Repeated X-ray measurements yielding identical spacing eliminated the possibility of water and toluene loss from the sample.

Results

DMPC Vesicles. The microscopical determinations of the elastic modulus k_c were performed using only freely fluctuating vesicles. The single vesicles were observed for several minutes and controlled for optically resolvable defects before acquisition of the contour coordinates.

Typical results of the analysis of contour fluctuations of a single pure DMPC vesicle are presented in Figure 2a. The

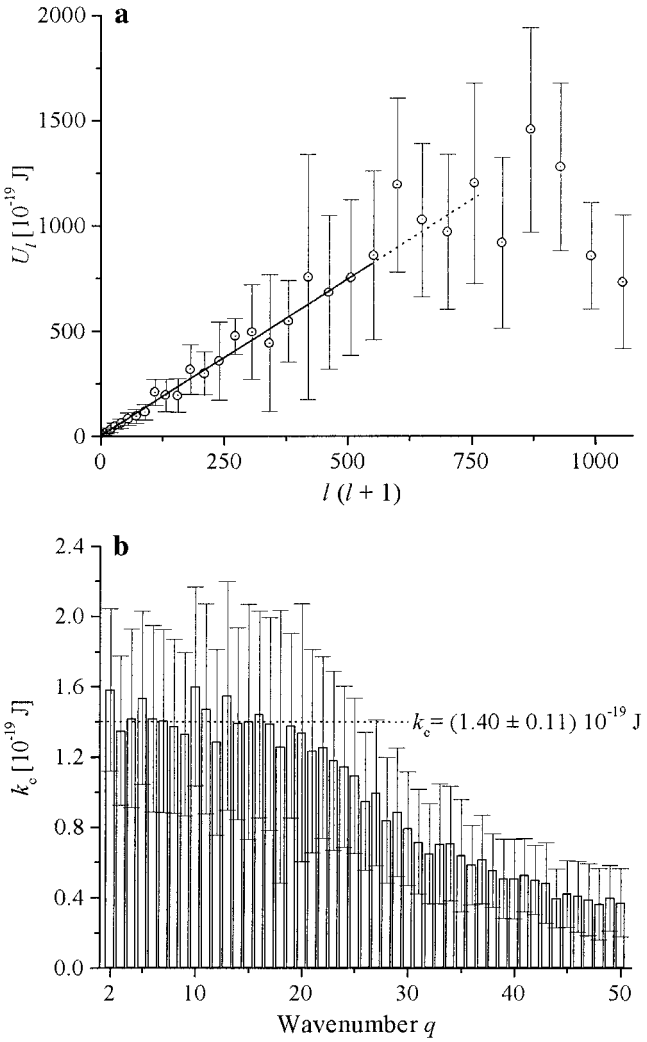

Figure 2. Analysis of the thermal fluctuations of 318 contours of a single fluctuating giant vesicle in dilute aqueous solution ($R_0 = 16.4$ μm, $\bar{\sigma} = 2 \pm 1$). (a) U_l vs $l(l + 1)$ plot for the determination of the bending elastic constant k_c and the effective tension $\bar{\sigma}$ following eq 9. The bending elastic constant can be deduced by a linear fit for $l < 22$, giving $k_c = (1.39 \pm 0.06) \times 10^{-19}$ J (solid line). Extrapolation of the line for $l > 22$ shows the deviation from the linear behavior (dotted line). (b) Plot of the bending elastic constant k_c as a function of the wavenumber q calculated from eq 3 and $\bar{\sigma} = 2$ obtained from the U_l vs $l(l + 1)$ plot. The values of k_c are independent of the wavenumber considered up to $q = 20$. From this plateau a mean value of $k_c = (1.40 \pm 0.11) \times 10^{-19}$ J can be obtained. Comparison of both methods gives a mean k_c of $(1.4 \pm 0.1) \times 10^{-19}$ J.

bending elastic constant is deduced by a linear fit of the data of the U_l vs $l(l + 1)$ plot, giving $k_c = (1.39 \pm 0.06) \times 10^{-19}$ J and $\bar{\sigma} = 2 \pm 1$. The value of the effective tension is further used as a fit parameter for the determination of the k_c vs q plot. The value of the bending elastic constant is indicated by the plateau value; for the data of Figure 2b $k_c = (1.40 \pm 0.11) \times 10^{-19}$ J. An alternative analysis with an effective tension $\bar{\sigma} = 0$ leads to a slightly larger value of k_c and a less extended plateau region with an increase of the bending elastic constant values at wavenumbers $q \leq 5$ (data not shown).

The deviation from the linear dependence of U_l vs $l(l + 1)$ for high order l as well as the apparent decay of k_c vs q is related to experimental limitations of the time and spatial resolution. A detailed analysis showed that the integration time of the videocamera is the first limiting factor.[45] The time-dependent behavior of the fluctuations is described by a time-dependent dynamic autocorrelation function. It can be decomposed as a series of Legendre polynomials with amplitudes $B_l(t,\bar{\sigma},k_c)$ relaxing according to[34,45]

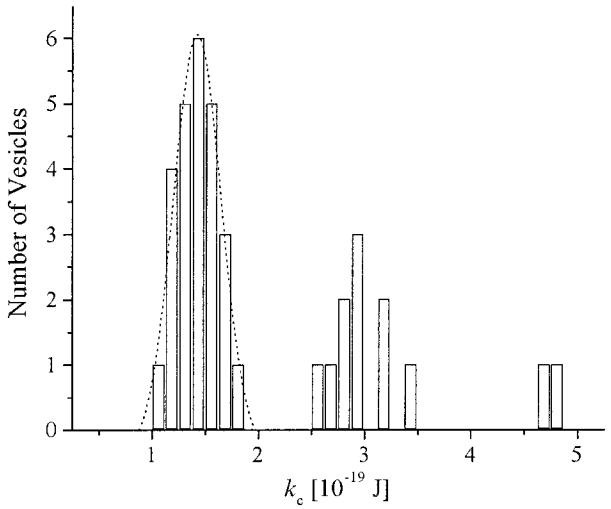

Figure 3. Histogram of the values of the bending elastic constant k_c obtained from 37 DMPC vesicles at 30 °C. The three Gaussian distributions indicate vesicles with different numbers of lamellae. The maximum of the first distribution holds a value of $k_c = (1.42 \pm 0.21) \times 10^{-19}$ J. This constant describes the bending elastic modulus of unilamellar vesicles.

$$B_l(t+\tau,\bar{\sigma},k_c) = B_l(t,\bar{\sigma},k_c)\, e^{-\tau/\tau_l} \tag{11}$$

The relaxation time τ_l for a given order l follows

$$\tau_l = \frac{\eta R_0^3}{k_c} \frac{2l+1}{(l+2)(l-1)[\bar{\sigma} + l(l+1)]} \frac{2l^2+2l-1}{l(l+1)} \tag{12}$$

where η is the viscosity of the aqueous phase.

If the integration time of the videocamera exceeds the relaxation time, the measured amplitudes become smaller than the real ones. This effect depends strongly on the vesicle size and leads to overestimated k_c values. The cutoff values for l can be evaluated by comparing the camera integration time with the relaxation time obtained from eq 12.

For the data of Figure 2a it turns out that the relaxation time becomes comparable with the camera integration time of 10 ms for $l = 22$. This is in fairly good agreement with the experimental findings showing a cutoff for $l = 23$. The slope of the curve then becomes larger, indicating an increase in the observed bending elastic constant. The decrease of the bending elastic constant observed for $l > 30$ is attributed to the restricted optical resolution of the microscope.[31]

Because the modes obtained by using a Fourier decomposition of the contour are a combination of the spherical harmonics, a similar relationship is expected for the correlation time τ_q of the amplitudes of the Fourier decomposition.[45] The data from Figure 2b indicate that a cutoff occurs at a wavenumber $q > 20$. This threshold value is in good agreement with the theoretically predicted limit. For larger wavenumbers q the modes are coupled and the representation shows a decrease of the bending elastic constant with q.

A large amount of giant vesicles must be analyzed in order to distinguish between the intrinsic property of the membrane and the particular behavior of single vesicles. The values of the bending elastic modulus of 37 DMPC vesicles are summarized in Figure 3. The peak corresponding to the lowest bending elastic constant is characteristic for single bilayer vesicles. These vesicles typically exhibit effective tensions

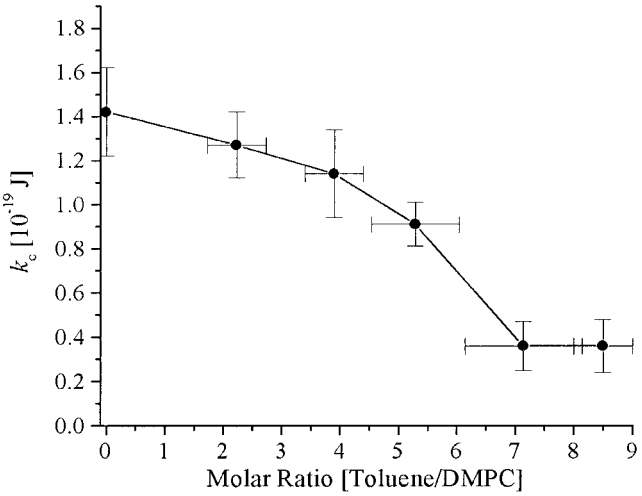

Figure 4. Influence of toluene on the bending rigidity of unilamellar DMPC vesicles (1 mM) at 30 °C. Average values are calculated by analyzing about 5−15 vesicles. The molar ratio represents the approximated concentration within the membrane as described in the text.

between $\bar{\sigma} = -4$ and 15. By fitting the data with a Gaussian distribution, one obtains the value of the bending elastic constant of unilamellar DMPC vesicles: $k_c = (1.42 \pm 0.21) \times 10^{-19}$ J. This value agrees reasonably well with those reported in the literature which lie between $k_c = 1.1 \times 10^{-19}$ and 2×10^{-19} J.[23,46] The scattering between the reported moduli is likely to be due to a strong dependence on the preparation method and the data treatment procedure.

Because the bending elastic constant is directly correlated to the membrane thickness, the higher values are supposed to be due to the oligolamellar vesicles which were beyond the limit of resolution of the optical device. This seems to be the case for bilamellar vesicles. Higher values may also be due to a deviation from the equilibrium conditions (i.e., $\Delta p \neq 0$) as indicated by the observation of a hysteresis of k_c during variation of the temperature.

Effect of Toluene on the Elastic Properties. The solubilization capacity for small aromatic molecules was shown to be considerably large.[47] Thus, the study of the influence of toluene on the bending elasticity could be performed over a wide range of compositions. Figure 4 represents the bending elastic constant as a function of toluene concentration. Three different regimes can be distinguished. For low toluene concentration only a weak variation of the bending modulus is observable. When the concentration is increased, the decay of k_c becomes faster until it finally levels off in the third region, where the water phase is completely toluene-saturated. The bending elastic modulus seems therewith to be independent of the toluene concentration. Creaming of the vesicles is also observed in this regime, indicating the lower density of the binary mixture.

Because for pure phospholipids the bending elastic modulus was shown to be predominantly controlled by the lipophilic part of the bilayer,[14] each modification of the interaction of the acyl moiety should have dramatic effects on k_c. Hence, the faint decrease of the bending elastic modulus in the first regime was quite unexpected. The presence of a plateau for the bending elastic constant for the third regime is also puzzling.

For toluene concentrations near the saturation limit of the membrane, vesicles exhibited a peculiar aspect: a homogeneously distributed amount of defects in the membrane region becomes visible under the microscope (Figure 5). These defects could be identified as clusterlike enrichments of the solute in the membrane. A fluctuation analysis of these vesicles leads to

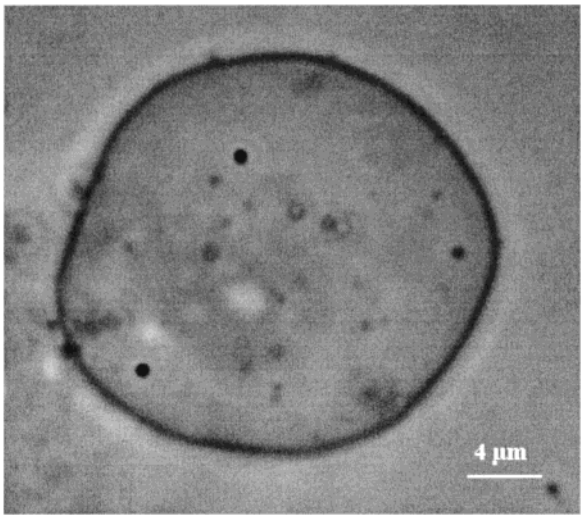

Figure 5. Snapshot of a fluctuating vesicle at toluene concentrations close to the maximum solubilization capacity of the DMPC membrane. The dark spots, usually homogeneously distributed, are situated at the vesicle surface. They characterize enrichments of the solute in the membrane region, which were often associated with microbudlike protrusions. The defects were stable during an observation time of a few hours. The cluster size was about 800 nm in diameter.

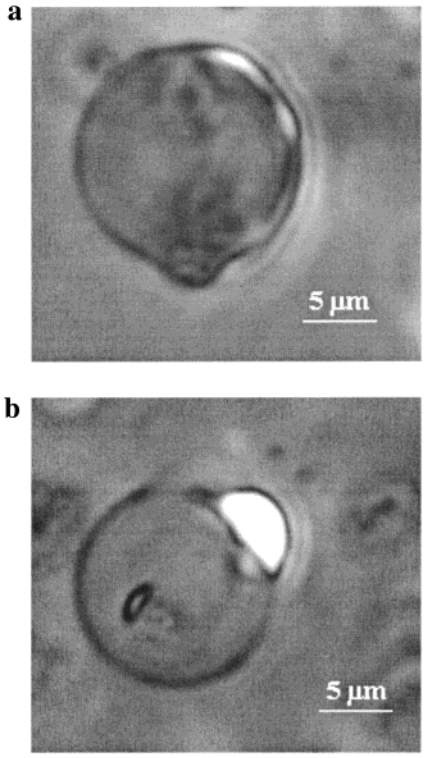

Figure 6. Nearly spherical DMPC vesicles at the maximum solubilization capacity. The vesicles contain large amounts of toluene in the bilayer region (bright areas). Under these conditions toluene becomes clearly visible using videomicroscopy.

$k_c = 1.0 \times 10^{-19}$ J, which corresponds to an increase in k_c. Nevertheless, the validity of the analysis of a vesicle with observable defects is questionable.

At toluene concentration above the maximum solubilization capacity, oil droplets coexist in the vicinity of spherical toluene-containing vesicles as reported for DPPC vesicles.[39] These vesicles exhibit phase-separated toluene in large cluster sizes (Figure 6), indicating the escape of the bilayer-incorporated toluene phase into the third dimension by wedging the two

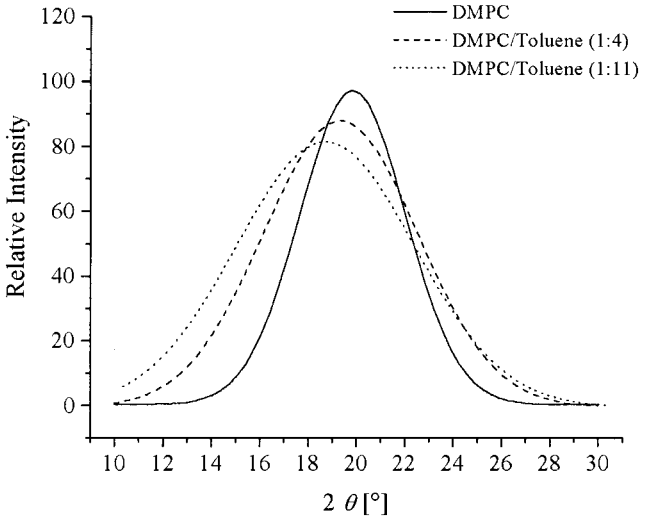

Figure 7. Wide-angle diffraction pattern of DMPC lamellar phases at different molar ratios of toluene/DMPC.

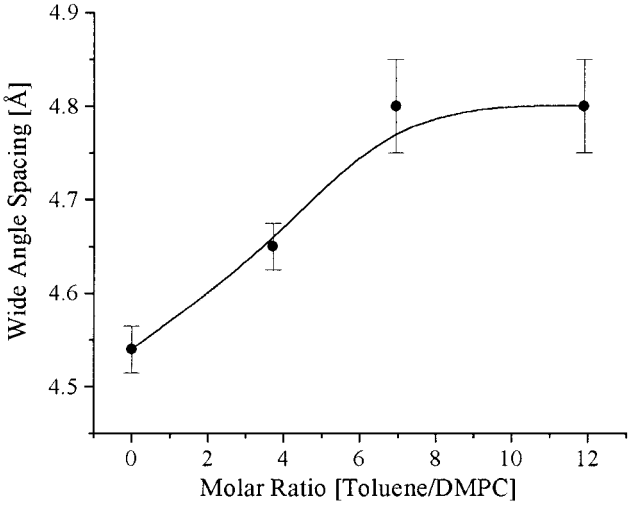

Figure 8. Wide-angle spacing as a function of the toluene/DMPC molar ratio indicating the increasing effective mean chain distance.

monolayers apart. To avoid the energetically unfavorable water/toluene contact, a large amount of phospholipid is needed. This reduces the excess area of the vesicle; thus, these vesicles do not exhibit any trace of thermal excited undulations. A similar phase separation can be observed for benzene/DMPC vesicles at the maximum solubilization capacity.

X-ray Diffraction. The molecular interaction of toluene with multilayers of phosphatidylcholine was studied at constant lipid/water ratios. Wide-angle diffraction peaks are shown for different toluene/lipid molar ratios in Figure 7. Two characteristic features can be distinguished at increasing toluene concentrations: the peaks become broader and their maxima shift toward smaller Bragg angles. The broadening is probably due to the enhancement of the fluctuations of the bilayers in the L_α phase. This phenomenon is typical for low-dimensionality phases. It is characterized by a power law behavior of the X-ray intensity.

For wavevectors parallel (||) and perpendicular (⊥) to the layers, one has respectively[48]

$$I(q_\perp=0,q_{||}) \propto 1/|q_{||} - q_0|^{2-\eta_c} \tag{13}$$

$$I(q_\perp,q_{||}=0) \propto 1/q_\perp^{4-2\eta_c} \tag{14}$$

where q_0 is the wavevector corresponding to the modulation and η_c is an exponent related to the compression elastic constant and to the bending elastic constant by

$$\eta_c \propto 1/\sqrt{Bk_c} \tag{15}$$

This power law behavior has already been observed for other compounds.[32,49]

The shift of the maximum of the peaks indicates a variation of the mean interchain distance. The latter has been reported in Figure 8. For increasing toluene/lipid molar ratios, the mean acyl-chain distance grows until it reaches a plateau value for toluene/lipid molar ratios of approximately 7. This result clearly indicates that toluene strongly interacts with the acyl moiety of the lipid by deeply penetrating into the lipophilic core of the bilayer and perturbing its structure. This, in turn, leads to a looser packing of the amphiphiles in the bilayer and an increase of the packing parameter.

Small-angle data were analyzed according to Lei.[50] The membrane thickness d_l of liquid-crystalline DMPC multilayers with the sample density ρ_s is obtained using

$$d_l = d_0 - d_w \tag{16}$$

where d_0 represents the repeat period obtained from small-angle diffraction. The water layer thickness d_w is given by

$$d_w = d_0 \frac{m_w}{m_s} \frac{\rho_s}{\rho_w} \tag{17}$$

where m_w and m_s are the mass of water and the total sample mass, respectively.

The results show an increase of the bilayer thickness from d_l = 3.5 nm of the pure DMPC bilayer up to 4.5 nm of the completely toluene-saturated DMPC membranes. This seems to be in good agreement with results obtained for benzene liquid-crystalline DLPC bilayers at 70 wt % water.[47] It is interesting to note that these authors did not observe a wide-angle peak shift.

By considering the whole X-ray patterns, one notes that no new peaks emerge even for high toluene concentrations. This indicates that no new ordered phase appears.

Thermotropic and Thermoelastic Properties of the Bilayer. The shapes of vesicles and their fluctuations are governed by curvature energy as well as geometrical parameters. The latter are constant volume V and area A. An increase in the temperature leads to an increase in A and to a reduction of the effective chain length l_c of the acyl chains. This furthermore decreases the bending rigidity.[14,22]

Examination of the thermotropic behavior was achieved in the vicinity of infinite dilution conditions. Characterization of the temperature dependence of k_c was performed using pure DMPC and DMPC/toluene vesicles. Because it is known that the membrane tension is also modified by temperature, only vesicles with similar effective tension were compared. The influence of the temperature on the bending elastic modulus is shown in Figure 9 respectively for a single DMPC and for a toluene-containing DMPC vesicle.

The thermal variation of the bending elastic constant is strongly affected by the incorporation of toluene into the lipophilic part of DMPC vesicles. In a temperature range between 29 and 31 °C, the decrease of k_c is twice as large as that in the absence of toluene.

Another important thermodynamic property to gain further insight into the structure of the lipid aggregates is the thermal

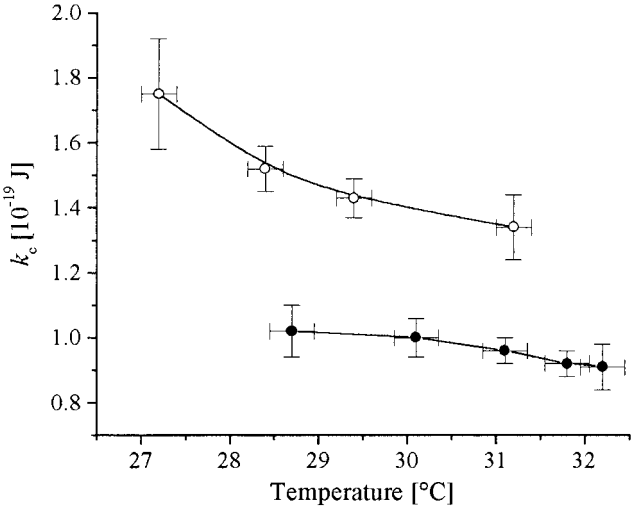

Figure 9. Effect of the variation of the temperature on the bending elastic modulus k_c of a single DMPC vesicle (−○−) and a toluene-containing DMPC vesicle near the maximum solubilization capacity (−●−). The molar ratio toluene/DMPC is approximately 5.

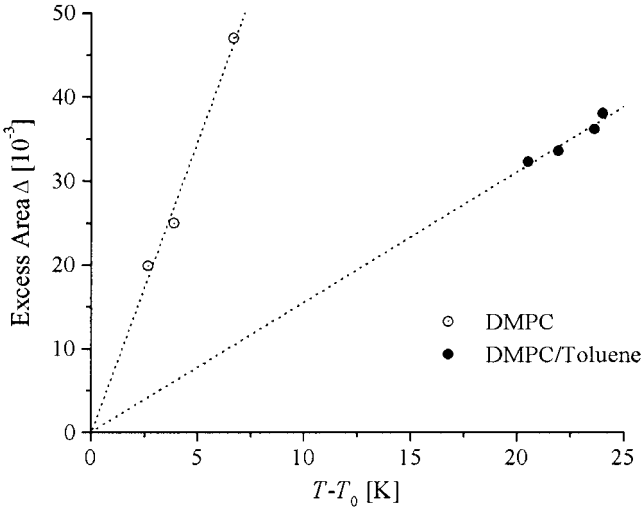

Figure 10. Plot of the excess area as function of the reduced temperature ($T - T_0$) in order to determine the thermal area expansion coefficient β. Δ is assumed to increase nearly linearly with temperature within the temperature range considered.

expansion coefficient. Because thermal expansivity of lipid bilayers is known to be anisotropic, distinction must be made between the area and volume expansion coefficients.[51] The latter is the sum of the area and the thickness expansion coefficient of the membrane. Thus, lateral expansion with increasing temperature should be accompanied by a simultaneous decrease of the membrane thickness.

Using microscopy techniques, it is possible to determine the area expansion coefficient β of single, unilamellar vesicles[31,52] given by

$$\beta = \frac{1}{A_0}\left(\frac{\partial A}{\partial T}\right)_p \tag{18}$$

From the temperature dependence of the effective tension and the bending elastic modulus, it is possible to determine the area expansion coefficient β by analyzing the temperature dependence of the excess area Δ[31] (Figure 10):

$$\Delta T = \beta(T - T_0) \tag{19}$$

TABLE 1. Values of T_0 and Thermal Area Expansion Coefficient β for Pure DMPC and Toluene-Containing DMPC Vesicles

	T_0 [°C]	β [10^{-3} K^{-1}]
DMPC	24.5	6.9 ± 0.8 (30 °C)
DMPC/toluene (1:5)	8.2	1.6 ± 0.3 (30 °C)

T_0 describes the temperature where the excess area vanishes ($\Delta = 0$). For this temperature thermal undulations disappear. The obtained values are shown in Table 1.

The results for a pure unilamellar DMPC vesicle are in good agreement with those presented in the literature. These lie between 6.8×10^{-3} K^{-1} at 29 °C[20] and 10.4×10^{-3} K^{-1} at 24 °C.[31]

The decrease of the thermal area expansivity in the presence of toluene at nearly maximum solubilization capacity is of the same order as that observed with DMPC/cholesterol mixtures at 50 mol %.[52]

Discussion

X-ray diffraction results indicate that toluene is predominantly incorporated in the lipophilic part of the bilayer. These observations are in good agreement with previous studies. It is known that alkanes[12,53] and small aromatic substances such as benzene[47] or toluene[39,54] are likely to be located in the acyl moiety of the lipid, hence increasing the area per lipid molecule.[55]

The solubilization capacity of the small aromatic molecules seems to be significantly high.[10,47] The lipophilic membrane core offers enough free volume to allow the incorporation of low amounts of small molecules in the fluid phase without notable perturbation of the bilayer.[56] A homogeneous distribution of toluene molecules in the fluid membrane is therefore favored. This is in good agreement with the small decrease of the bending elasticity observed in the low toluene regime which may be due to reduced acyl−acyl interactions. Under these dilute conditions a transfer of toluene into the waterphase becomes possible because of its finite solubility. Hence, one may also consider a coupling mechanism arising from the escape of toluene from the denser regions of the locally highly curved membrane into the waterphase.

When the concentration is increased, diffusion of the toluene molecule in the membrane may influence the bending elastic modulus. In contrast to polar additives anchored in the headgroup region of fluid vesicles, nonpolar substances exhibit a high lateral mobility. Typical diffusion constants are on the order of $D = 1.1 \times 10^{-6}$ cm^2 s^{-1} for benzene, 0.5×10^{-6} cm^2 s^{-1} for naphthalene,[57] and 2×10^{-7} cm^2 s^{-1} for pyrene.[58] These values are about 10 times higher than those obtained for fatty acids.[57] Furthermore, there is strong evidence that even stiff molecules such as pyrene show mobility in the transmembrane direction.[59] We shall consider two cases: lateral (*in plane*) and transmembrane (*transversal*) diffusion, both effects leading to local concentration gradients in the membrane. Lateral diffusion seems to strongly influence the value of the bending elastic constant in the case of surface-active molecules.[27,32,36] Because the regions of higher curvature offer better packing conditions, the intercalated molecules will diffuse laterally into these regions. This diffusion process is much faster than the out-of-plane-fluctuations; therefore, the bending elastic constant will diminish. In the case of lipophilic substances, such a mechanism is likely to occur in the membrane because the small toluene molecule can diffuse easily in plane.

In the case of lipophilic molecules, transmembrane diffusion is also possible. During the undulation one monolayer is locally

compressed whereas the other is expanded. The transmembrane diffusion of toluene causes an enrichment of the small molecules in the expanded monolayer. The amplitudes of the fluctuations will then be enhanced. Both coupling mechanisms between concentration and elastic energy share the same geometrical origin. However, the theories cited before cannot be used because transmembrane diffusion may induce a variation of the chemical potential of the monolayer.

For high concentrations the system reaches a critical concentration where demixing into toluene-rich and lipid-rich domains might take place. A similar behavior was observed from high-sensitivity differential scanning calorimetry (DSC) for DPPC/cholesterol mixtures.[60] It seems, therefore, possible that phase composition fluctuation induced by this phase transition will contribute to the lowering of the bending elastic constant over this whole range of concentrations. Such pretransitional effects are known to strongly affect the compressibility of two-component mixtures.[61] A similar effect is expected for the bending elastic modulus of membranes.[62,63]

At toluene concentrations near the maximum solubilization capacity of the membrane, k_c reaches a plateau value. At this concentration the water phase is completely saturated with toluene, and no further escape of molecules into the water phase is possible. Therefore, one could assume that this phenomenon is related to the complete decoupling of the molecules in the layer. This would follow a screening of acyl−acyl interactions due to the complete swelling of the acyl moiety. The decoupling effect can be detected by DSC measurements and has already been observed for benzene/DSPC mixtures[47] and by ^{1}H NMR titration experiments.[39] X-ray diffraction patterns also support this hypothesis because they show an increase of the wide-angle spacing.

The bending elastic behavior is not dominated by the bilayer thickness because it is known for the pure system.[14] The thickening observed indicates that the two opposing monolayers are decoupled. Therefore, a possible hindrance of the mutual slip[44] cannot be envisaged at high concentrations.

At the maximum solubilization capacity, the membrane becomes inhomogeneous. Small protrusions stable over the time period of the observation do appear. They originate from the phase separation which occurs for these high concentrations. Toluene enriches in the form of small clusters in the membrane. The observed cluster size in Figure 5 is about 800 nm in diameter. A similar effect of local enrichment in the membrane has been observed at off-critical concentrations for dynamic simulations of vesicles.[63]

The vesicles presenting these defects were associated with anomalous high bending rigidity. This may be related to the gradual disappearance of the excess area Δ because more and more phospholipids molecules are needed in order to avoid oil−water contact. When the excess area has completely disappeared, the vesicles stop fluctuating.

Acknowledgment. Financial support of this work by grants of the Deutsche Forschungsgemeinschaft (SFB 1690), Fonds der Chemischen Industrie, and the Forschungspool of the University of Essen is gratefully acknowledged. We thank U. Seifert and H.-G. Doebereiner (MPI for Colloids and Interfaces, Golm) for stimulating and fruitful discussions.

References and Notes

(1) Lasic, D. D. *Liposomes: From Physics to Applications*; Elsevier: Amsterdam, The Netherlands, 1993.
(2) Barenholz, Y.; Lasic, D. D. *Handbook of Nonmedical Applications of Liposomes*; CRC Press: Boca Raton, FL, 1996.
(3) Seifert, U. *Adv. Phys.* **1997**, *46*, 13.
(4) Lipowsky, R.; Sackmann, E. *Structure and dynamic of membranes*; Elsevier: Amsterdam, The Netherlands, 1995; Vol 1.
(5) Johannsson, A.; Keightley, C. A.; Smith, G. A.; Richards, C. D.; Hesketh, T. R.; Metcalfe, J. C. *J. Biol. Chem.* **1981**, *256*, 1643.
(6) Suwalsky, M.; Benites, M.; Villena, F.; Aguilar, F.; Sotomayor, C. P. *Biochim. Biophys. Acta* **1996**, *1285*, 267.
(7) Gregoriadis, G. *Liposome Technology*; CRC Press: Boca Raton, FL, 1983.
(8) Murtagh, J.; Thomas, J. K. *Faraday Discuss. Chem. Soc.* **1986**, *81*, 127.
(9) Hotz, J.; Meier, W. *Adv. Mater.* **1998**, *10*, 1387.
(10) Kurja, J.; Nolte, R.; Maxwell, J. M.; German, I. A. *Polymer* **1993**, *34*, 2045.
(11) Hotz, J.; Meier, W. *Langmuir* **1998**, *14*, 1031.
(12) McIntosh, T. J.; Simon, S. A.; MacDonald, R. C. *Biochim. Biophys. Acta* **1980**, *597*, 445.
(13) Faucon, J. F.; Mitov, M. D.; Méléard, P.; Bivas, I.; Bothorel, P. *J. Phys. Fr.* **1989**, *50*, 2389.
(14) Fernandez-Puente, L.; Bivas, I.; Mitov, M. D.; Méléard, P. *Europhys. Lett.* **1994**, *28*, 181.
(15) Kummrow, M.; Helfrich, W. *Phys. Rev. A* **1991**, *44*, 8356.
(16) Bivas, I.; Hanusse, P.; Bothorel, P.; Lalanne, J.; Aguerre-Chariol, O. *J. Phys.* **1987**, *48*, 855.
(17) Helfrich, W. *Z. Naturforsch.* **1978**, *33A*, 305.
(18) Bailey, S. M.; Chiruvolu, S.; Israelachvili, J. N.; Zasadzinski, J. A. N. *Langmuir* **1990**, *6*, 1326.
(19) Cevc, G.; Gebauer, D.; Stiebner, J.; Schätzlein, A.; Blume, G. *Biochim. Biophys. Acta* **1998**, *1368*, 201.
(20) Evans, E.; Needham, D. *J. Phys. Chem.* **1987**, *91*, 4219.
(21) Bo, L.; Waugh, R. E. *Biophys. J.* **1989**, *55*, 509.
(22) Niggemann, G.; Kummrow, M.; Helfrich, W. *J. Phys. II* **1995**, *5*, 413.
(23) Schneider, M. B.; Jenkins, J. T.; Webb, W. W. *J. Phys.* **1984**, *45*, 1457.
(24) Safinya, C. R.; Sirota, E. B.; Roux, D.; Smith, G. S. *Phys. Rev. Lett.* **1989**, *62*, 1134.
(25) Engelhardt, H.; Duwe, H. P.; Sackmann, E. *J. Phys. Lett.* **1985**, *46*, L-395.
(26) Méléard, P.; Gerbeaud, C.; Pott, T.; Fernandez-Puente, L.; Bivas, I.; Mitov, M. D.; Dufourcq, J.; Bothorel, P. *Biophys. J.* **1997**, *72*, 2616.
(27) Szleifer, I.; Kramer, D.; Ben-Shaul, A.; Gelbart, W. M.; Safran, S. A. *J. Chem. Phys.* **1990**, *92*, 6800.
(28) Szleifer, I.; Kramer, D.; Ben-Shaul, A.; Roux, D.; Gelbart, W. M. *Phys. Rev. Lett.* **1988**, *60*, 1966.
(29) Duwe, H. P.; Sackmann, E. *Phys. A* **1990**, *163*, 410.
(30) Duwe, H. P.; Käs, J.; Sackmann, E. *J. Phys. Fr.* **1990**, *51*, 945.
(31) Häckl, W.; Seifert, U.; Sackmann, E. *J. Phys. II* **1997**, *7*, 1141.
(32) Leibler, S. *J. Phys. Fr.* **1986**, *47*, 507.
(33) Cevc, G.; Blume, G.; Schätzlein, A. *J. Control Relat.* **1997**, *45*, 211.
(34) Milner, S. T.; Safran, S. A. *Phys. Rev. A* **1987**, *36*, 4371.
(35) Faucon, J. F.; Méléard, P.; Mitov, M. D.; Bivas, I.; Bothorel, P. *Prog. Colloid Polym. Sci.* **1989**, *79*, 11.
(36) Seifert, U. *Z. Phys. B* **1995**, *97*, 299.
(37) Bivas, I.; Bilvolarski, L.; Mitov, M. D.; Derzhanski, A. *J. Phys. II Fr.* **1992**, *2*, 1423.
(38) Reeves, J. P.; Dowben, R. M. *J. Cell. Physiol.* **1969**, *73*, 49.
(39) Brückner, E.; Rehage, H. *Prog. Colloid Polym. Sci.* **1831**, *109*, 21.
(40) Angelova, M. I.; Soleau, S.; Méléard, P.; Faucon, J. F.; Bothorel, P. *Prog. Colloid Polym. Sci.* **1992**, *89*, 127.
(41) Lewis, R. N. A. H.; Mak, N.; McElhaney, R. N. *Biochemistry* **1987**, *26*, 6118.
(42) Mitov, M. D.; Faucon, J. F.; Méléard, P.; Bothorel, P. *Advances in Supramolecular Chemistry. A Research Annual* in *Thermal Fluctuations of Membranes*; JAI Press Inc.: Greenwich, CT, 1992; Vol. 2, p 93.
(43) Liu, H. K. *CGIP* **1977**, *6*, 123.
(44) Katz, Y.; Diamond, J. M. *J. Membr. Biol.* **1974**, *17*, 69.
(45) Méléard, P.; Mitov, M. D.; Faucon, J. F.; Bothorel, P. *Europhys. Lett.* **1990**, *11*, 355.
(46) Duwe, H. P.; Engelhardt, H.; Zilker, A.; Sackmann, E. *Mol. Cryst. Liq. Cryst.* **1987**, *1*, 152.
(47) McDaniel, R. V.; Simon, S. A.; McIntosh, T. J.; Borovyagin, V. *Biochemistry* **1982**, *21*, 4116.
(48) Caillé, A. *C. R. Acad. Sci. B* **1972**, *274*, 891.
(49) Roux, D.; Safinya, C. R. *J. Phys. Fr.* **1988**, *49*, 307.
(50) Lei, N.; Lei, X. *Langmuir* **1998**, *14*, 2155.
(51) Raudino, A.; Zuccarello, F.; La Rosa, C.; Buemi, G. *J. Phys. Chem.* **1990**, *94*, 4217.
(52) Needham, D.; McIntosh, T. J.; Evans, E. *Biochemistry* **1988**, *27*, 4668.
(53) White, S. H.; King, G. I.; Cain, J. E. *Nature* **1981**, *290*, 161.

(54) Gusev, D. G.; Vasilenko, I. A.; Evstigneeva, R. P. *Biol. Membr.* **1990**, *3*, 1038.
(55) Lea, E. J. A. *Int. J. Biol. Macromol.* **1979**, *1*, 185.
(56) Antunes-Madeira, M. C.; Madeira, V. M. C. *Biochim. Biophys. Acta* **1989**, *982*, 161.
(57) Rigaud, J. L.; Gary-Bobo, C. M.; Sanson, A.; Ptak, M. *Chem. Phys. Lipids* **1977**, *18*, 23.
(58) Galla, H.-J.; Sackmann, E. *Biochim. Biophys. Acta* **1974**, *339*, 103.
(59) Vekshin, N. L. *J. Biochem. Biophys. Methods* **1987**, *15*, 97.
(60) McMullen, T. P. W.; McElhaney, R. N. *Biochim. Biophys. Acta* **1995**, *1234*, 90.
(61) Pippard, A. B. *Philos. Mag.* **1956**, *1*, 473.
(62) MacKintosh, F. C.; Safran, S. A. *Phys. Rev. E* **1993**, *47*, 1180.
(63) Taniguchi, T.; Kawasaki, K.; Andelman, D.; Kawakatsu, T. *J. Phys. II Fr.* **1994**, *4*, 1333.